Development of Predictive Geoarchaeological Models to Locate and Assess the Preservation Potential of Submerged Prehistoric Sites Using Remote Sensing, Palaeoenvironmental Analysis, and GIS

David John Gregory [1,*], **Ole Bennike** [2], **Jørn Bo Jensen** [2] , **Peter Rasmussen** [1] **and Zyad Al-Hamdani** [2]

[1] Section for Environmental Archaeology and Materials Science, The National Museum of Denmark, I.C. Modewegs Vej, Brede, 2800 Copenhagen, Denmark; peter.rasmussen@natmus.dk
[2] Geological Survey of Denmark and Greenland, C.F. Møllers Allé 8, 8000 Aarhus, Denmark; obe@geus.dk (O.B.); jbj@geus.dk (J.B.J.); azk@geus.dk (Z.A.-H.)
[*] Correspondence: david.john.gregory@natmus.dk

Abstract: Using the Mesolithic site of Tudse Hage in the Great Belt of Denmark, this paper proposes a generic stepwise process to create geoarchaeological models that output seamless morphology maps in a GIS. This was achieved using remote sensing databases and the collection of marine geophysical data, above and below the seabed. On the basis of these data, key areas, with sediment sequences representative of the postglacial transgression surfaces, were identified. Core samples were taken for palaeoenvironmental analysis and dating that enabled a reconstruction of the relative sea-level changes. Using this information, palaeogeographic coastline maps of the Kongemose, late Kongemose, Ertebølle, and Neolithic periods in the Tudse Hage area were prepared, and potential hotspots for archaeological sites were proposed. Since their inundation, submerged prehistoric archaeological sites have been, and are, dynamic, with anthropogenic and natural processes affecting their stability and preservation. With the advocation of in situ preservation as a means of managing underwater cultural heritage, predicting where sites have survived these processes, and where they can be found, in advance of subsea development or other anthropogenic exploitation, is essential. Future natural threats to sites preserved in situ were determined through the modelling of seabed currents and sediment erosion.

Keywords: palaeoenvironmental analyses; remote sensing; GIS; relative sea-level change; submerged prehistoric archaeology; in situ preservation

1. Introduction

1.1. Predictive Modelling to Locate Submerged Prehistoric Sites and Landscapes

The fishing-site-location model is a method that was pioneered by Anders Fischer in the 1980s and 1990s to locate submerged prehistoric sites [1–3]. It stems from his observations that the location of coastal prehistoric sites in Denmark correlated well with the locations of modern day "hobby" fishermen [4] p. 54. The coastal landscape affects where fish and eels swim and where they can be trapped or caught. His hypothesis was that "settlements were placed on the shore immediately beside good sites for trap fishery. Such places were at the mouths of streams, at narrows in the fjord and on small islands and promontories close to sloping bottoms in the fjord" [1] p. 6. This was initially tested through diving and reconnaissance in the Småland Bight in Denmark using a three-phase approach: (1) Map plotting; (2) Localisation and delimitation of sites by echosounder; and (3) Marking of the theoretical site with a marker buoy, followed by diving to investigate. Key to testing was the use of the available information on the Quaternary geology, coastal morphology, and seafloor sedimentary conditions of the places under study in order to focus on areas that were relatively unaffected by erosion and/or sedimentation.

In the intervening years, there have been robust critiques of the "Danish" model, notably by Benjamin [5] and Grøn [6]. Benjamin expands Fischer's original three-phase approach to six phases. Benjamin's Phase 1 includes regional familiarization with archaeology, geography, geology, geomorphology, oceanography, and hydrology. Phase two includes the need to include and understand the ethnographic component, including cultural parallels, historical research, and modern interviews. Grøn's critique draws on the fact that the fish-site-location model uses outdated landscape ecology modelling and that modelling attempts, such as Fischer's, are based on assumptions about prehistoric resources-strategic behaviour that are oversimplistic and similarly outdated. Nevertheless, we believe that determining which Holocene deposits survive and reconstructing palaeocoastlines are important first goals in attempting to predict where sites are. As the marine environment has been, and still is, dynamic, from the time of a site's inundation, it will have been affected by a range of postdepositional cultural and natural formation processes. It is thus imperative to know both what has survived, and what will survive in the future. As Benjamin and commentators to his 2010 article have discussed, there has been a significant development in remote sensing techniques, such as satellite imagery, LIDAR, multibeam echosounding, and sub-bottom profiling, since Fischer's groundbreaking work. Similarly, the advent of Geographical Information Systems has enabled the presentation and analysis of complex datasets. These factors, coupled with the ever-increasing amount of online open-access data, make the generation of palaeogeographic maps easier than has hitherto been possible.

1.2. In Situ Preservation and the Management of Underwater Cultural Heritage

Danish [7], European [8] and international law [9,10] all advocate that, where possible, underwater archaeological sites should be preserved in situ where they lie. In part, this is due to the sheer amount of underwater cultural heritage. For example, it has been estimated that about 20,000 submerged archaeological settlements, and the same number of shipwrecks, lie in Danish territorial waters [11]. However, in situ preservation should not be a case of leaving a site where it is and hoping that it will be there when archaeologists and conservators have the capacity, research questions, and desire to investigate these finds in the future. Rule 4 of the UNESCO Convention Annex states that "the in situ preservation of underwater cultural heritage (i.e., in its original location on the seafloor) should be considered as the first option before allowing or engaging in any further activities. The recovery of objects may, however, be authorized for the purpose of making a significant contribution to the protection or knowledge of underwater cultural heritage." Although the sentiment is admirable, in situ preservation is not a panacea and is not always feasible. The authors have previously discussed that there are five fundamental steps to ensuring the successful and informed management of underwater archaeological sites in situ [12]:

1. The location and extent of the site to be preserved, both on and in the seabed;
2. The most significant physical, chemical, and biological threats to the site;
3. The types of materials present on the site and their state of preservation;
4. Strategies to mitigate deterioration and stabilise sites. Depending upon the environment and location of the sites, it may be sufficiently benign that the site can be preserved in situ or, in certain cases, it is more responsible to excavate a site in order to prevent its total loss;
5. The subsequent monitoring of a site and any implemented mitigation strategies.

This paper discusses the approaches taken to Points 1 and 2, using the Mesolithic site and the area around Tudse Hage in Denmark as a case study. The research was conducted as part of the European project, SASMAP: Development of Tools and Techniques to Survey, Assess, Stabilise, Monitor and Preserve Underwater Archaeological Sites (2012–2016). For the reader's interest, information concerning Points 3–5 is available in [13] and on the SASMAP project website (www.sasmap.eu accessed on 7 December 2021).

1.3. Tudse Hage: Holocene History of The Study Area

During the last ice age, the world sea level was about 130 m lower than at present, and the last glaciation of the Tudse Hage region (Figure 1) saw glaciers come from the south or the southeast. The area is dominated by clay-rich glacial till, but there are also a few small occurrences of clay that were deposited in glacial lakes. As the ice sheets in North America and northern Europe disappeared, the sea level rose. In Denmark, the land also rose because it had been freed from an immense weight, but in the Tudse Hage area, the sea-level rise surpassed the land uplift. At the end of the last glaciation, subglacial meltwater eroded deep valleys in the Great Belt region [14]. These valleys were partly filled by sediments after the last deglaciation, which probably occurred about 17 ka years ago [15]. In the earliest Holocene, the water level was approximately 25 m lower in the region than present-day water levels, and mires developed, even in the deeper parts of the valleys. However, increasing water levels in the early Holocene led to the drowning of these mires and to the formation of large lakes. During the continued shore-level rise, the water became brackish and, later, marine. Marine bivalves and gastropods invaded the region, and the oldest reported radiocarbon age of a shell of a marine mollusc from the Great Belt is 8.2 cal. ka BP [16]. The relative sea level culminated during the mid-Holocene and reached a level around 0.75 m above the present level [17]. Hence, we now find submerged settlements and in situ tree stumps, as well as lake and mire deposits, below the present sea level. At Tudse Hage, several Mesolithic sites have been located from the Ertebølle culture, mainly in shallow water, but there have also been a few in somewhat deeper water, about 5.5 m, from the late Kongemose culture. The Ertebølle sites are located in a shallow-water area, with till and boulders on the sea floor. Submerged archaeological finds were made during dredging in the area in the 1890s. In 1957, a submerged Mesolithic site was found in shallow waters by divers, and artefacts of wood were later found [18–20].
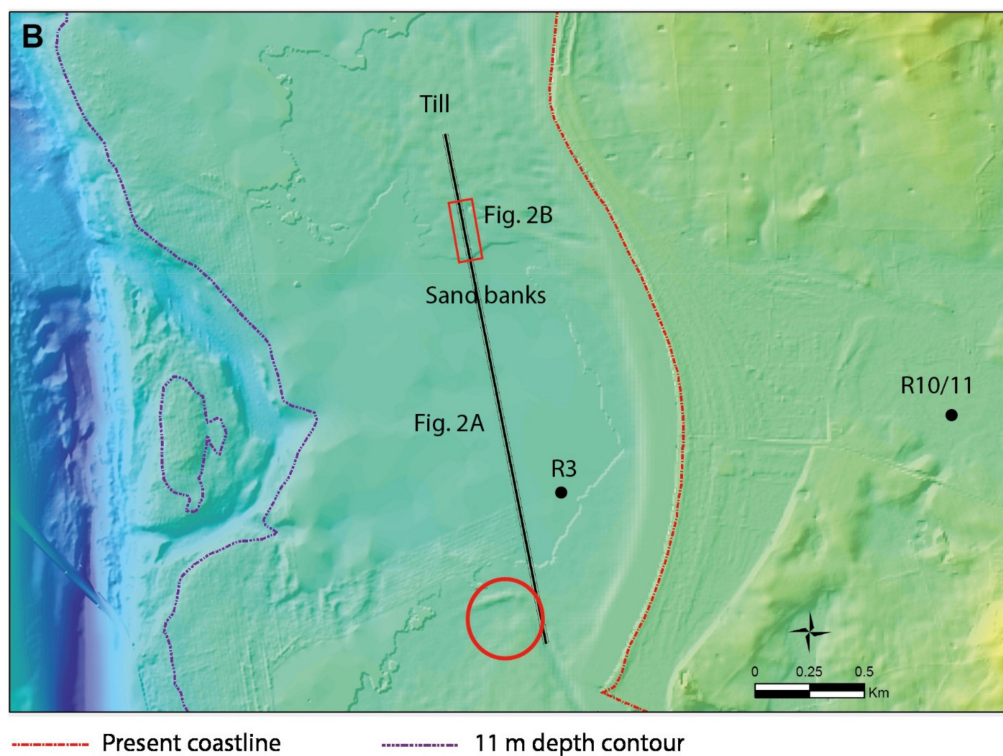

Figure 1. *Cont.*

Figure 1. (**A**) Orthophoto of the Tudse Hage area. The inset map shows the location of the Tudse Hage area in Denmark. The red circle shows the location of the Mesolithic finds in situ. The white dashed line shows the location of the profile in Figure 2A, and the red rectangle shows the location of the seismic profile in Figure 2B. (**B**) Seamless map of the Tudse Hage area, showing flat topography. The map is based on LIDAR data and multibeam echosounder data. The red circle shows the location of the Mesolithic finds in situ. The black dots show the location of the Russian cores, Rus 3 (R3), Rus 10, and Rus 11 (R10/11).
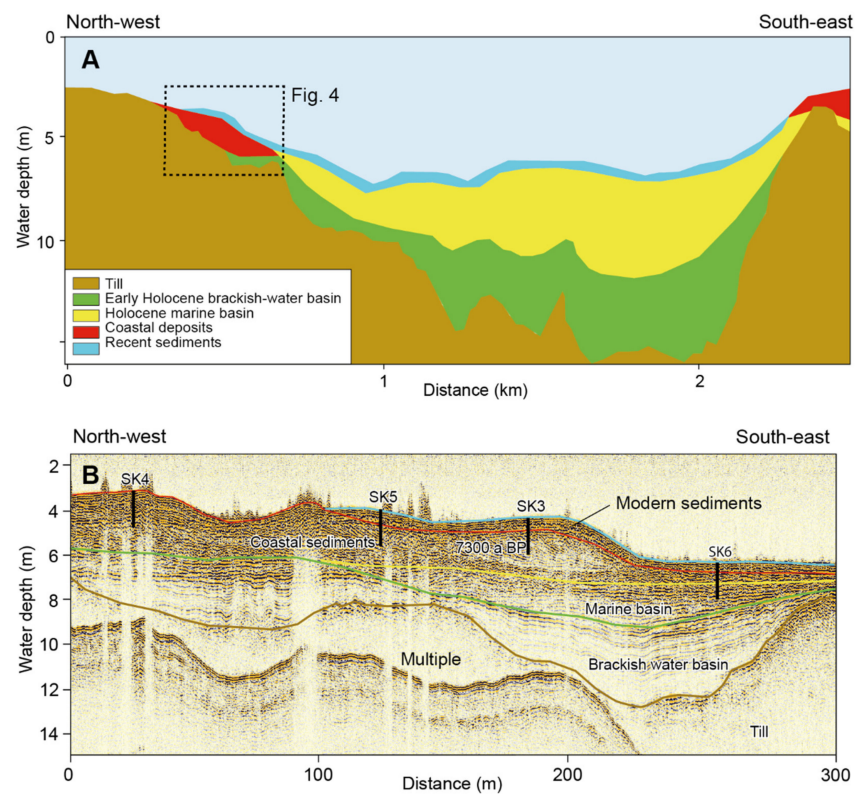

Figure 2. (**A**) Profile across the survey area at Tudse Hage, with glacial till that is partly covered by

Holocene and recent sediments. The location of the profile is indicated on Figures 1 and 2A. The profile is based on interpretation of seismic data. (**B**) Profile acquired with an Innomar parametric sub-bottom profiler. The profile crosses drowned coastal sediments that are dated to c. 7.4 cal. ka BP. The location of the profile is indicated on Figures 1 and 2A.

2. Methods

2.1. The Downscaling and Upscaling Concept

Environmental studies typically involve the combination of several dynamic models with many different data sources. The spatial and temporal scales at which these models operate are often very different from each other. Moreover, the scale at which available data have been collected is usually different from the scale required by the models. To overcome this scale discrepancy, a vast body of different methods has been developed to transfer the data and model output from a larger to a smaller scale (downscaling), or from a smaller to a larger scale (upscaling) [21]. The downscaling concept can be seen as starting from the "big picture", whereby remote sensing techniques, i.e., very large-scale satellite, orthophoto, or LIDAR images are investigated, and the major morphological structures and their distributions are delineated. Both satellite bathymetry and ortho/satellite morphology are used to design the field work areas that can provide the best "zoom in" datasets for the model production. In the next stage, a geophysical survey is conducted in the areas identified in the previous step; this has the advantages of producing the exact data required to fulfil the work requirements, reducing the processing time, and remarkably decreasing the survey time and the subsequent, diving, sampling, and ground-truthing. Processing and interpreting the geophysical data, both seismic side-scan images and bathymetry, reveals locations where ground-truth sampling, or coring, should be taken for the calibration of the acoustic data and for obtaining other parameters that the acoustic survey cannot provide, such as a sediment size analysis to classify the seabed type, and samples for dating. The latter is important for any sea-level-change calculation, geological model enhancing, and calibration. The starting point of the SASMAP project was to use the downscaling and upscaling approach to both locate potential submerged prehistoric sites and assess their future preservation potential in the area of Tudse Hage, Denmark. The specific workflow to achieve this is described in the following sections.

2.2. Downscaling

1. The generation of seamless morphology maps in a GIS platform over the entire area, using satellite, LIDAR, and orthophoto remote sensing databases;
2. Marine geophysical survey using multi- and single-beam echosounders, side-scan sonar, and a sub-bottom profiler.

2.3. Upscaling

1. On the basis of the maps and profiles generated, key areas were selected for core sampling to obtain sedimentological, biostratigraphic, and chronological data;
2. These three steps enabled the elucidation of the paleogeographical evolution (sedimentary conditions and water-level fluctuations) and the paleoenvironment of the area through time. This step importantly identifies the seabed areas that have survived or, conversely, that have been eroded away since the time of inundation, which would thus negate the need for further investigation;
3. The production of geoarchaeological/paleogeographic maps of past coastlines and the identification of potential archaeological "hotspots", according to Fischer's (1993) fishing-site-location model;
4. The identification of erosive and sedimentary environments for future in situ management purposes.

2.4. Downscaling to Assess Paleogeographic Evolution (Steps 1–2)

Satellite images over the Tudse Hage area were purchased from DHI-GRAS A/S. The images were obtained by a Worldview-2 multispectral imagery satellite that has a spatial resolution of 1.8 m at nadir (transmitted wave axis normal to the ground surface) and ~2 m at 20° off-nadir. The topography of the adjacent onshore areas was mapped from LIDAR data (https://download.kortforsyningen.dk/ accessed on 7 December 2021). Both datasets were used to produce seamless maps in a GIS platform (ArcGIS), which showed the morphology of the area, both onshore and offshore. These maps formed the basis for defining specific areas for subsequent marine geophysical surveys, where the bathymetry of the deeper areas was determined by multibeam echosounding, and the surface seabed sediments were classified and mapped using side-scan sonar and subsurface sediments and sediment stratigraphy mapped with a sub-bottom profiler. The side-scan sonar results were used to generate acoustic image mosaics that could identify any natural and/or archaeological objects lying proud of the seabed. The mosaics were ground-truthed and used to generate surface sediment maps, which assisted in the interpretation of the upper layer of the sub-bottom profiler data gathered using an Innomar SES-2000 parametric sub-bottom profiler. Again, these datasets were added to the GIS and enabled the selection of specific locations from which to take sediment cores for obtaining paleoenvironmental samples, as will be discussed. During the SASMAP project, a parametric sub-bottom profiler (SES2000-Quattro), capable of recording 3D profiles, was developed with the German project partner, Innomar. Unfortunately, it was not possible to use it on the site during the project, but it has subsequently been successfully used by other researchers to document sub-bottom strata and features on archaeological sites in 3D [22].

2.5. Upscaling through Paleoenvironmental Analyses and Reconstructing Relative Sea-Level Rise (Steps 3–5)

Coring was carried out using a Russian corer [23]; cores denoted Rus 3, Rus 10, and Rus 11) and a small diver-held vibracorer (cores denoted SK1–SK6, and a core TH of 2), developed as part of the SASMAP project by the Danish project partner, AKUT. Rus 10 and Rus 11 were collected on land from an area of raised marine deposits named Holmene, located ~1.8 km northwest of Skælskør, whereas the other cores were collected offshore. The locations of the cores are provided in Table 1. The offshore core positions were selected from the seismic profiles, and the onshore positions from the topography. The aim of the coring was to obtain material that covered as wide a time span as possible. The cores were described and logged. Subsamples from the cores were wet-sieved and analyzed for macrofossils. The ages of the selected macrofossils were determined by accelerator mass spectrometry radiocarbon dating at the AMS laboratory in Aarhus, Denmark, and at the Beta laboratory in Miami, Florida (Table 2). The ages of the samples of terrestrial plant remains were calibrated to calendar ka BP, using the INTCAL20 dataset, and the ages of marine shells were calibrated using the MARINE20 data. We used a ΔR value of −150 years for marine samples, corresponding to a reservoir age of 400 years.

2.6. Predictive Modelling of Preservation Potential (Step 6)

In estuarine and coastal areas, the seabed is in a state of constant dynamic change and understanding what effect this has on the postdepositional formation processes of sites is essential when attempting to both interpret and manage archaeological sites. One of the key parameters affecting the preservation of submerged prehistoric sites is seabed erosion. The main hydrodynamic parameter controlling erosion, suspension, and deposition is the bed shear-stress, which is the frictional force exerted by the flow of water per unit area of bed [24]. To assess the likelihood of seabed erosion, a 3D hydrodynamic model was developed by applying the MIKE 3 FM modelling tool [25]. The hydrodynamic model calculates the spatial and temporal variations of the current velocities, the surface elevation, as well as the temperature, salinity, and density of the water. The model is based on bathymetric data from the former Danish Maritime Safety Administration (Farvandsvæsnet), boundary

data from the encompassing FEHY models [26], and meteorological data from The Water Forecast by DHI. The general model has previously been calibrated and validated against measured data from the former Storstrøms County [27]. The multibeam echosounder data were used to refine the bathymetry of the area. The model was executed for a one-year period to represent the annual flow conditions. As the flow conditions in Tudse Hage are characterized by either north- or south-going currents, the statistical processing of the model results was designed to distinguish between these two flow situations. The model results were saved every hour during the one-year model simulation, and for each hour that the current-generated bed shear-stress calculated the modelled current velocity. The calculation of the current-generated bed shear-stress was made according to Soulsby and Clarke [24]. In the bed shear-stress calculation, the median grain diameter (d50) of the seabed was taken to be 0.1 mm, corresponding to fine-grained sand.

Table 1. Locations of sediment cores from the Tudse Hage area, southern Great Belt, Denmark.

Core	Latitude N	Longitude E	Water Depth (cm)	Elevation (cm)
Onshore				
Rus 10	55°15.701′	11°15.867′		24
Rus 11	55°15.735′	11°15.704′		19
Offshore				
Rus 3	55°15.484′	11°14.187′	630	
SK 1	55°15.314′	11°13.956′	500	
SK 2	55°15.295′	11°13.982′	450	
SK 3	55°16.119′	11°14.091′	450	
SK 4	55°16.170′	11°14.074′	370	
SK 5	55°16.138′	11°14.082′	430	
SK 6	55°16.088′	11°14.102′	550	
TH2	~55°15′	~11°14.175′		

3. Results

3.1. Downscaling to Assess Paleogeographic Evolution

The seamless map for the selected area centered around the Tudse Hage site is shown in Figure 1B. Most of the offshore area is characterized by shallow waters, but there is a distinct valley coming from the south and running first towards the north, and then towards the west. It was probably formed by subglacial meltwater during the last deglaciation. The central part of the Tudse Hage area is characterized by a flat bottom and basin sediments. To the north and south are areas with boulders and stones on the sea floor, which represent till surfaces with lag sediments. In the north, there are also some sand banks. Skælskør Nor and Skælskør Inderfjord are separated from the Storebælt by a relatively high area, with the highest hill reaching an elevation of 27 m above sea level; this area is dominated by glacial till (Jupiter – Denmark's geological and hydrological database; http://www.geus. dk/UK/data-maps/jupiter/Pages/default.aspx accessed on 7 December 2021). Between this high elevation area and the coast, there is a fossil lagoon and fossil beach ridges.

3.2. Upscaling through Paleoenvironmental Analyses and Reconstructing Relative Sea-Level Rise

Sediments

Several different sediment types are found in the Tudse Hage area (Figures 2 and 3). The oldest unit is glacial till. In sediment cores Rus 3, Rus 10, and Rus 11, we found sand with pebbles at the base; this is probably glaciofluvial sand. In the same sediment cores, a 10–20-cm-thick layer of peat is found. The peat in Rus 10 and Rus 11 is overlain by

clay-rich gyttja containing shells of marine molluscs. The marine gyttja is laminated with organic-rich laminae with some remains of terrestrial plants, including wood fragments (TH 2). In sediment core Rus 10, lacustrine gyttja is found above the marine gyttja, and in core Rus 3, lacustrine gyttja is found below the marine gyttja. Homogeneous or laminated sand and gravel with shells of marine molluscs are found in the vibracores; these sediments represent drowned coastal deposits.
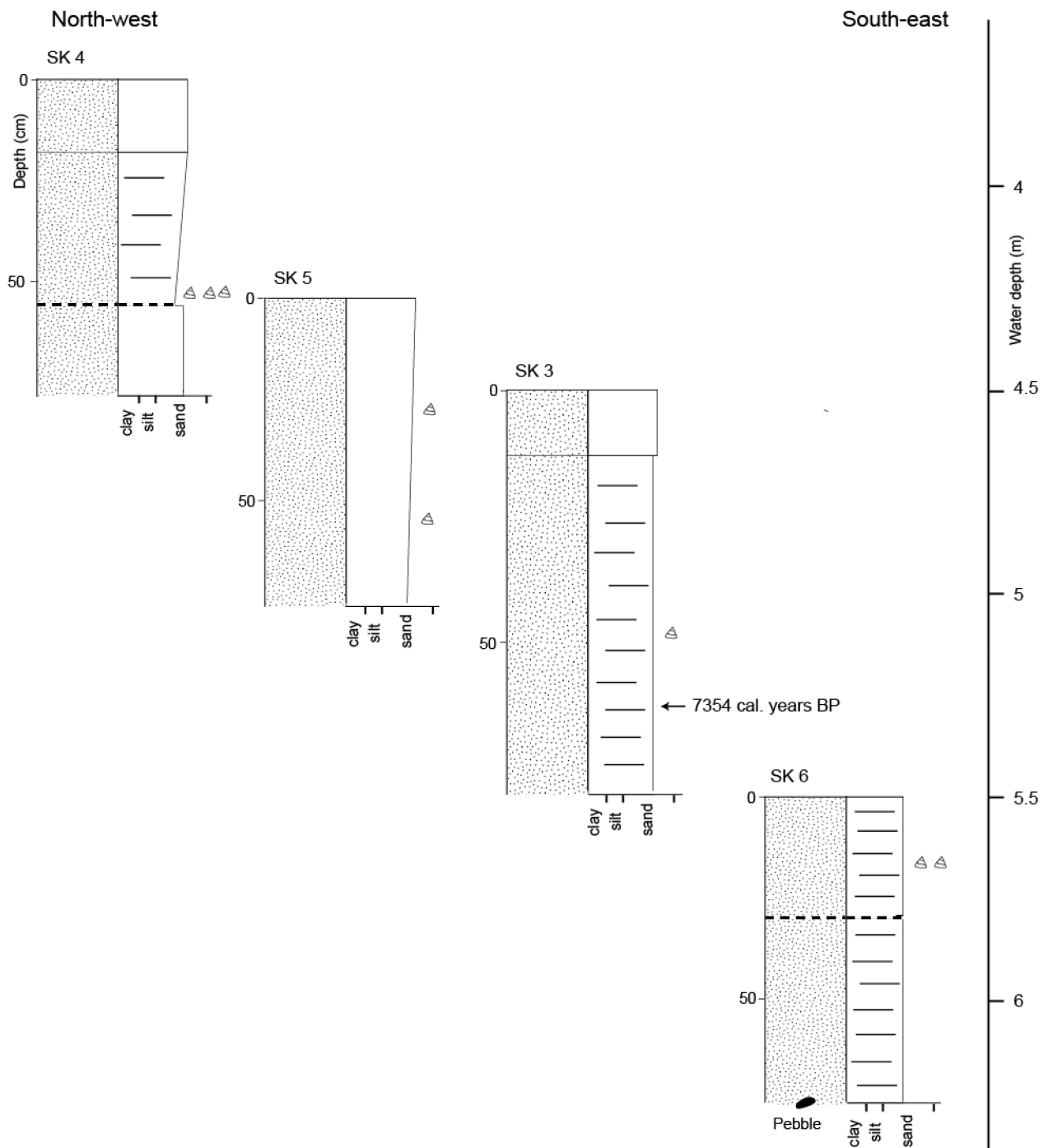

Figure 3. Sedimentological logs of the sediment cores, SK 4, 5, 3, and 6. For location, see Figure 2.

3.3. Macrofossils and Chronology

Offshore Cores

Rus 3 was collected offshore, at a water depth of 630 cm. The sediments consist of pebbly sand, clayey gyttja, and fine-grained sand. The macrofossil diagram from Rus 3 is divided visually into three biozones (Figure 4). The most common macrofossil in Zone 1 is the sclerotia of the soil fungus, *Cenococcum geophilum*. In addition, the remains of *Alnus glutinosa* are fairly common, whereas the fruits of *Scirpus lacustris* are rare. *Alnus glutinosa* and *Scirpus lacustris* indicate a wetland environment, and *Cenococcum geophilum* indicates pronounced soil erosion. The dating of the *Alnus* remains yielded an age of 8.5 cal. ka BP. Zone 2 is dominated by the shells and head shields of *Chydorus sphaericus,* and the head capsules of the larvae of Chironomidae indet. There were also statoblasts of *Cristatella mucedo* and the remains of the larvae of Trichoptera indet. These species show that the sediments were deposited in a freshwater lake, probably a small local lake. A sample of leaf fragments of deciduous trees was dated to 8.3 cal. ka BP. This age corresponds to the dating of the Kongemose culture in Denmark. The sediments belonging to Zone 3 contain a range of marine fossils. However, in the lowermost part, *Cerastoderma* sp. is the only mollusc present. This extremely low species diversity indicates brackish water conditions shortly after the initial marine transgression. One of the lowermost shells was dated to ~7.9 cal. ka BP. A bit higher up in the succession, the common blue mussel, *Mytilus edulis*, the small gastropod, *Hydrobia* sp., as well as foraminifers appear, followed by *Littorina littorea*, *Macoma balthica*, *Rissoa* spp. and *Parvicardium exiguum*. Still higher up in the succession, there is an interval with shells of the oyster, *Ostrea edulis*. The oldest occurrence of this species was dated to 7.1 cal. ka BP, and the youngest to 6.3 cal. ka BP. The occurrence of *Ostrea edulis* indicates high salinity and warm and nutrient-rich waters in the region. This time interval corresponds to the dating of the Ertebølle culture in Denmark. The radiocarbon ages of *Ostrea edulis* shells from Danish shell middens show a maximum of ages at about 6 cal. ka BP [28], somewhat later than the peak occurrence in Rus 3. Shells of *Ostrea edulis* are common in the Tudse Hage area, and the largest shells measure 7 cm [29]. The upper part of Zone 3 shows low diversity, indicating lowered salinity and the poor preservation of mollusc shells.

The lower part of SK 1 consists of laminated fine-grained organic-rich sediments, with *Cerastoderma* sp. and *Potamogeton pectinatus*, which indicate a shallow brackish-water environment. A shell sample was dated to ~7.7 cal. ka BP (Table 2). The sediment is also rich in charcoal, which is probably of anthropogenic origin. SK 2 also penetrated laminated fine-grained sediments with *Mytilus edulis*, *Cerastoderma* sp., *Hydrobia* sp., *Littorina saxatilis*, *Theodoxus fluviatilis*, *Chara* sp., *Perca fluviatilis*, *Tolypella* sp., *Potamogeton pectinatus*, *Ruppia* sp., *Zannichellia palustris,* and charcoal; this assemblage also indicates a shallow brackish-water environment. Two samples were dated to ~7.7 and 7.8 cal. ka BP. SK3 penetrated sandy sediments, with rare fragments of shells of *Mytilus edulis*, *Cerastoderma* sp., *Macoma balthica*, *Littorina littorea,* and *Mya* sp. One sample gave a modern age, and another was dated to ~7.3 cal. ka BP. The sediments in SK 4, SK 5, and SK 6 are similar to SK 3: the assemblages include *Pectinaria* sp., *Balanus* spp. and *Zostera* sp. Three dated samples gave modern ages. This could be because of the high sedimentation rates, but we consider it more likely that modern materials were brought downcore during the vibracoring. It is interesting to note that charcoal is common in the fine-grained sediments. We have no direct radiocarbon ages of the charcoal, but it can hardly be younger than the shells that yielded the ages of 7.7–7.8 cal. ka BP (Table 2). This indicates that the charcoal comes from fires by people from the younger part of the Kongemose culture.
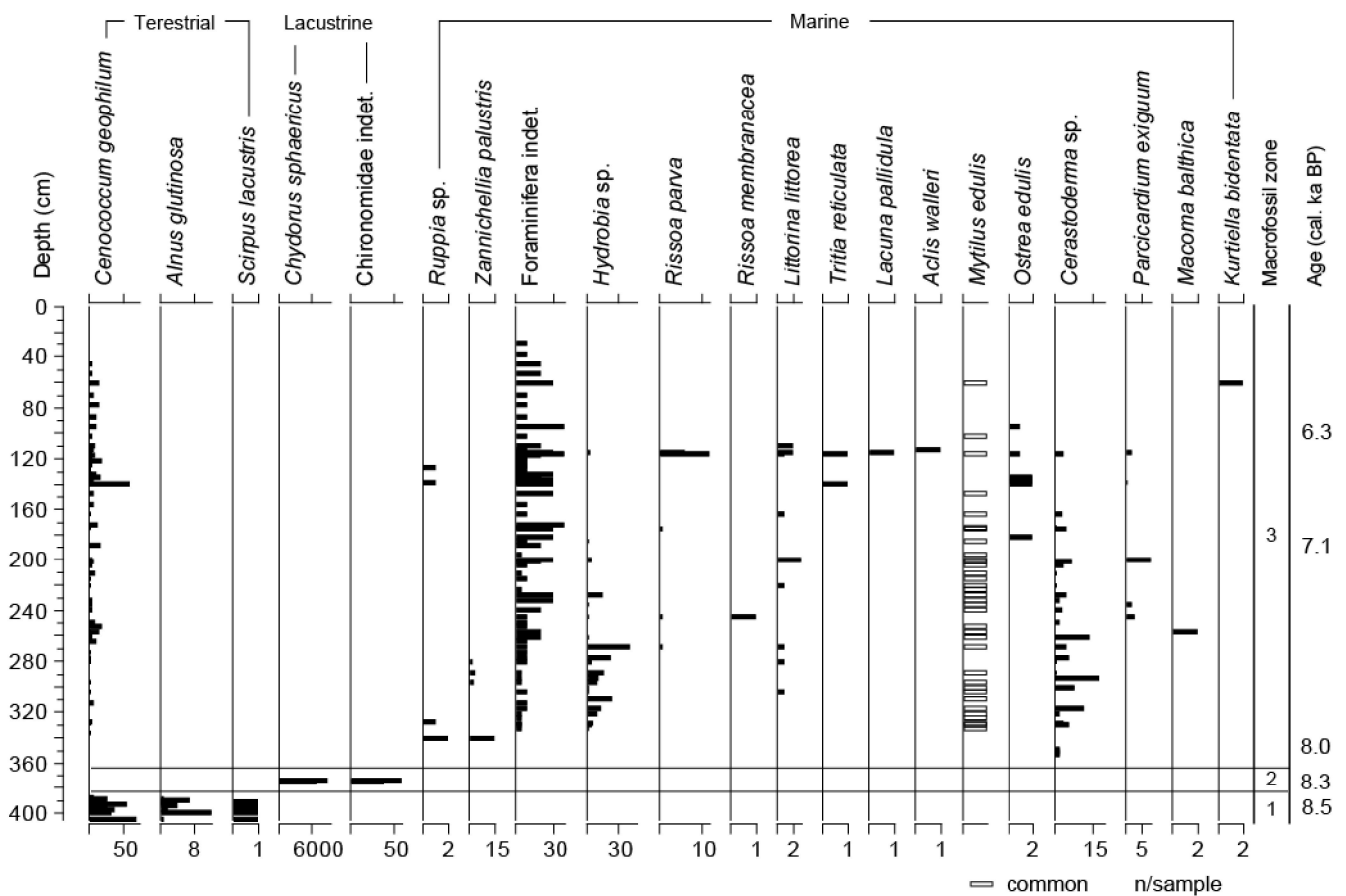
Figure 4. Simplified macrofossil concentration diagram for Rus 3, collected at 55°15.484′N, 11°14.187′E.

Table 2. Radiocarbon ages from the Tudse Hage area, Denmark.

Core	Lab. No.	Material	Depth bsl [1] (cm)	Age (^{14}C) yrs (BP) [2]	Calibrated age (BP) [3]	Calibrated age (BP) [4]
Rus 3	AAR-23210	*Ostrea edulis*	725–726	5890 ± 29	6115–6414	6270
Rus 3	AAR-23211	*Ostrea edulis*	812–813	6612 ± 31	6909–7236	7072
Rus 3	AAR-23212	*C. lamarcki*	982–983	7506 ± 40	7775–8097	7932
Rus 3	AAR-19918	Leaf fragments [5]	999–1003	7455 ± 50	8181–8371	8271
Rus 3	AAR-19919	*Alnus glutinosa*	1020–1021	7740 ± 75	8380–8697	8516
Rus 10	AAR-23213	Leaf fragments [5]	104–106	4230 ± 29	4649–4856	4811
Rus 10	AAR-23214	*C. lamarcki*	238–240	6543 ± 32	6821–7161	6998
Rus 10	AAR-23215	Plant remains	240–242	6538 ± 33	7339–7511	7456
Rus 11	AAR-23216	Leaf fragments [5]	86–87	5139 ± 48	5747–5994	5894
Rus 11	AAR-23217	Leaf fragments [5]	134–135	5888 ± 36	6632–6793	6709
Rus 11	AAR-23218	*C. lamarcki*	193–194	6381 ± 31	6643–6974	6807
Rus 11	AAR-23219	Leaf fragments [5]	209–210	6235 ± 29	7013–7253	7161
Rus 11	AAR-23220	*P. australis*	217–218	6225 ± 40	6999–7254	7108
Rus 11	AAR-23221	*Quercus* sp.	227–228	6500 ± 40	7318–7498	7382

Table 2. *Cont.*

Core	Lab. No.	Material	Depth	Age (^{14}C)	Calibrated	Calibrated
SK 1	AAR-21895	*C. lamarcki*	573–577	7284 ± 50	7558–7876	7713
SK 2	AAR-21896	*C. lamarcki*	490–500	7262 ± 50	7540–7859	7691
SK 2	AAR-21897	*C. lamarcki*	540–550	7363 ± 50	7629–7944	7790
SK 3	AAR-21898	*Mytilus edulis*	480–490	Modern		
SK 3	AAR-21899	*C. lamarcki*	510–520	6834 ± 50	7143–7454	7300
SK 4	AAR-21900	*Littorina littorea*	410–420	Modern		
SK 5	AAR-21901	*Mytilus edulis*	440–450	Modern		
SK 6	AAR-21902	*Littorina littorea*	575–585	Modern		
TH 2	Beta-385200	Wood	218	6000 ± 30	6746–6936	6838
TH 2	Beta-385201	*Corylus* wood	223	6220 ± 30	7003–7250	7098
TH 2	Beta-385202	Wood	233	6110 ± 30	6893–7156	6981
TH 2	Beta-385203	*Corylus* wood	248	6220 ± 30	7003–7250	7098
TH 2	Beta-385204	*Corylus* wood	266	6430 ± 30	7280–7423	7361
Artefacts						
Oar	K-6605	*Tilia* wood	*c.* 200	6230 ± 80	6908–7318	7117
Ax handle	Ua-2496	*Corylus* wood	*c.* 225	5305 ± 75	5928–6276	6091

[1] bsl: below sea level. [2] Radiocarbon ages are reported in conventional radiocarbon years, BP (before present = 1950; [30]). The ^{14}C ages have been corrected for isotopic fractionation to a δ^{13}C value of –25 ‰. [3] Calibration to calendar years BP is according to the INTCAL20 and MARINE20 data [31,32]. For marine samples, we used a reservoir age of 400 years. [4] Mean probability ages. [5] Leaf fragments of deciduous trees.

3.4. Onshore Cores

Rus 10 was collected at an elevation of 24 cm above sea level, as determined from the LIDAR data. The sediments consisted of pebbly sand, peat, and gyttja, with the macrofossil diagram divided into four biozones (Figure 5). Zone 1 is characterized by the abundant remains of the reed plant, *Phragmites australis*. In addition to *P. australis*, there are many sclerotia of the soil fungus, *Cenococcum geophilum*, and rare remains of *Cornus sanguinea* and *Corylus avellana*. The transgression of the area led to a rising of the groundwater table and the area became covered by reed beds. The occurrence of *C. geophilum* indicates soil erosion.

Zone 2 is characterized by marine macrofossils, but the lower part of this zone is extremely species-poor, with the marine bivalve, *Cerastoderma lamarcki,* and the aquatic plant, *Ruppia* sp., as the only species. The species composition and the low diversity indicate brackish water conditions. Higher up in Zone 2, the diversity increases, and shells of the blue mussel, *Mytilus edulis*, and a small number of gastropods, such as *Hydrobia* sp. and *Rissoa parva*, appear, as well as the polychaete worm, *Nereis* sp. and Hydroidea indet. *Ruppia* sp. fruits are common in the upper part of the zone, and in the uppermost part of the zone, shells of *Littorina littorea* appear; this species indicates that firm substrates were present. A shell from the bottom of Zone 2 was dated to 7.0 cal. ka BP. The assemblages in Zone 2 indicate a shallow-water marine environment, with a somewhat restricted connection to the sea. In Zone 3, only a few shells and shell fragments of molluscs are found, and *Ruppia* sp. is rare. *Nereis* sp. is still rare but is present in many of the samples analyzed. At around an 80-cm depth, there is a small peak of the terrestrial plant, *Atriplex* sp. This plant is common on beaches, especially at places with a high organic content, as is found in areas where the remains of aquatic macrophytes accumulate. The Zone 3 assemblages indicate brackish water conditions, with a strongly diminished connection to the sea as compared with Zone 2. A sample from the bottom of Zone 3 was dated to 4.8 cal. ka BP.

In Zone 4, shells of the gastropod, *Radix balthica* (= *Lymnaea peregra*), appear; this is a freshwater species that can cope with slightly brackish conditions. It occurs together with *Cerastoderma lamarcki*, *Nereis* sp. and *Chara* sp., which can also tolerate brackish conditions. In the uppermost sample, *Radix balthica* occurs together with *Hippuris vulgaris*, and the local environment is now completely fresh—as it is today.
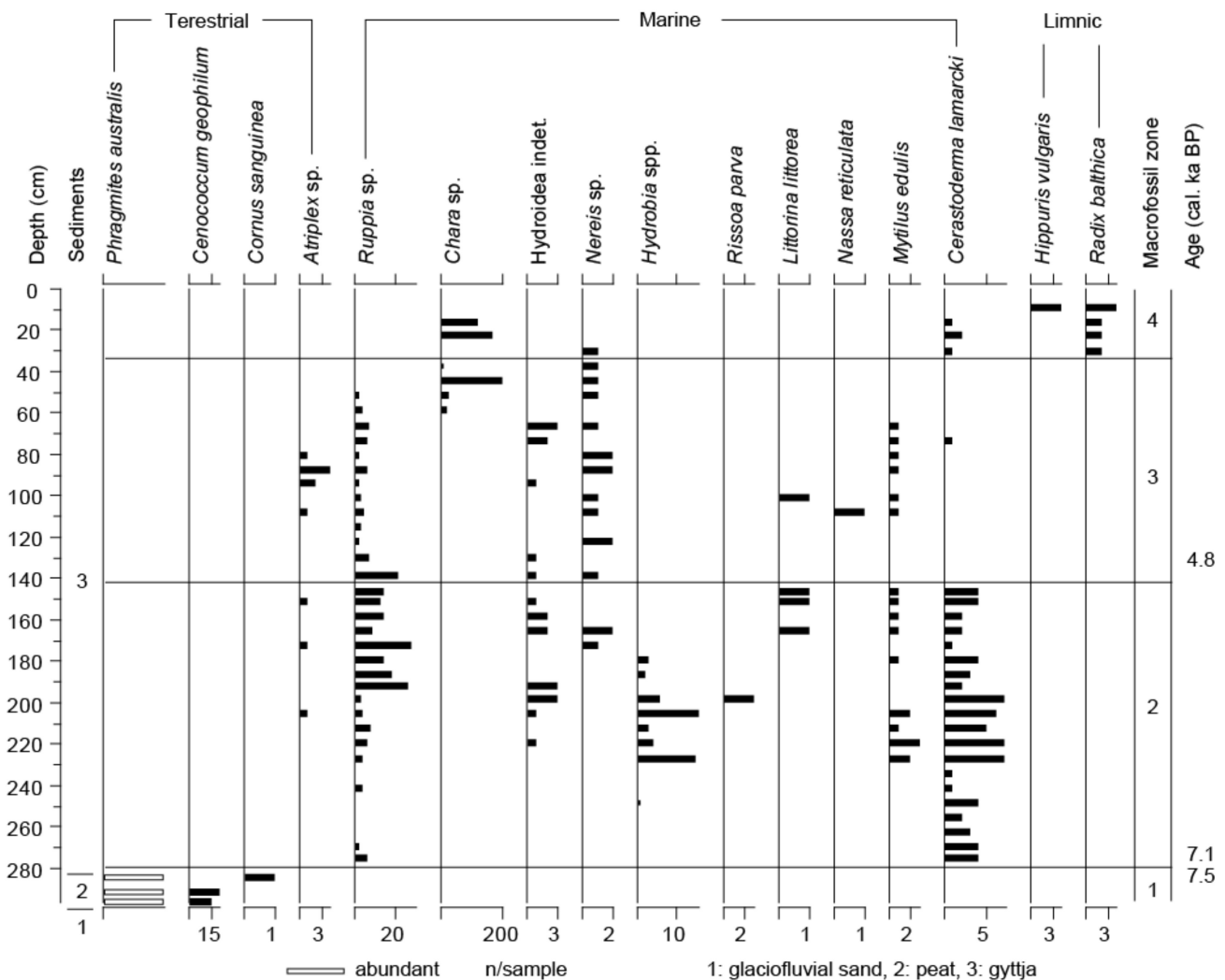

Figure 5. Simplified macrofossil concentration diagram for Rus 10.

Rus 11 was collected at an elevation of 19 cm above sea level, as determined from the LIDAR data. The sediments consist of pebbly sand, peat, and gyttja, with the macrofossil diagram divided into three biozones (Figure 6). However, the upper part of the succession was not sampled. Zone 1 is characterized by the abundant remains of *Phragmites australis*, indicating the local presence of reed beds. Two samples of terrestrial plant remains were dated to 7.4 and 7.1 cal. ka BP. Zone 2 is characterized by abundant tests of an agglutinating foraminifer, tentatively identified as *Trochammina* sp. and by the linings of calcareous foraminifers. No remains of molluscs were found in this zone. The lack of molluscs, and the low diversity of marine fossils, indicate brackish water conditions. A sample of terrestrial plant remains from the upper part of Zone 2 was dated to 7.2 cal. ka BP. The lack of this zone in Rus 10 may indicate that some sediments were removed from the Rus 10 core site by erosion during the marine transgression. In Zone 3, shells of marine bivalves (*Cerastoderma lamarcki* and *Mytilus edulis*) and marine gastropods (*Hydrobia* sp., *Littorina littorea* and *Rissoa* spp.), rare jaws of *Nereis* sp., rare remains of Hydroidea indet.

and fruits of *Ruppia* sp. are found, indicating a shallow-water marine environment that was connected to the Great Belt. A shell from the bottom of Zone 3 was dated to 6.8 cal. ka BP, slightly younger than in core Rus 10, which may reflect that the oldest shell in Rus 11 occurred at a slightly higher level than in Rus 10. A sample from the middle part of Zone 3 was dated to 6.7 cal. ka BP, and a sample from the upper part of Zone 3 was dated to 5.9 cal. ka BP. The uppermost sample contains no shells of marine molluscs; this could be because of the dissolution of the carbonate shells or decreased salinity. *Ruppia* sp. is fairly common. The assemblages indicate that the salinity decreased at the coring site in the mid-Holocene, perhaps because the water depth decreased as the small basin was filled by sediments.

Figure 6. Simplified macrofossil concentration diagram for Rus 11.

4. Discussion

4.1. Summary of the Geological Evolution

Till and pebbly sand were deposited during the last ice age. A layer of peat formed during the transgression of the area, probably from the accumulation of reed plants. The presence of lacustrine gyttja in core Rus 3 shows that a lake existed at the core site during the early part of the transgression; it was presumably a local lake that formed in a local depression. After the transgression of the area, brackish-water and marine gyttja accumulated in relatively deep water, and sandy and gravelly deposits accumulated in the coastal zone, at a time when the relative sea level was ~3 m lower than at present. Hence, the sandy and gravelly deposits represent drowned sediments.

4.2. Reconstructing Relative Sea-Level History

Figure 7 shows the radiocarbon ages plotted versus the mean sea level. The green samples represent terrestrial sediments, and the blue samples come from marine sediments. The solid line shows a proposed relative sea-level curve for the Tudse Hage area. The lower and upper parts of the curve are well-constrained from both terrestrial and marine ages, whereas the middle part is poorly constrained. We see evidence for an unconformity in

the area, which could be due to a low stand, which may have occurred c. 7.6 cal. ka BP, during a time period when the curve is poorly constrained from radiocarbon ages. The dashed line in the diagram shows a relative sea-level curve for the Halskov area, which is located 13–14 km north of the Tudse Hage area [33]. The older part of the Halskov curve fits the data from Tudse Hage well, but, in the younger part, it can be seen that terrestrial samples from Tudse Hage plot below the Halskov curve. This difference may be because of real differences in the sea-level histories between the two areas, or because of uncertainties in dating, or uncertainties about the elevation of the dated samples. The main dating uncertainty relates to the local reservoir effects for marine shell samples. Reservoir ages may vary over relatively short distances [34]. However, we consider such uncertainties to be too small to account for the observed differences. Christensen et al. [33] suggest that alternating low stands and high stands occurred in the Halskov area, but these are younger than the low stand suggested for the Tudse Hage area. The dotted line shows a relative sea-level curve for southern Lillebælt [35]. The area is located about 95 km west of Tudse Hage. The older part of this curve also fit the data from the Tudse Hage area, but marine samples from the area from depths of 5–6 m plot above the curve. This shows that the glacioisostatic rebound was more pronounced in the Tudse Hage and Halskov areas than in southern Lillebælt. As mentioned, Christensen et al. [33] did not find evidence for a low stand at 7.6 cal. ka BP, but Christensen [36] suggests that the relative sea rose slowly, during a short time interval, at around 7.5 cal. ka BP.
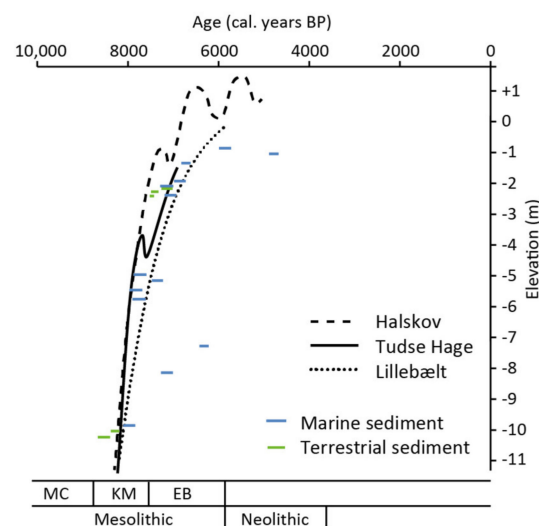

Figure 7. Relative sea-level changes in the Tudse Hage area. MC: Maglemose culture. KM: Konge-mose culture. EB: Ertebølle culture.

4.3. Generation of Geoarchaeological Paleogeographical Maps

During the Holocene transgression of the area, more and more land was covered by the sea. Figure 8 shows an example of a paleogeographical map at a time when the sea level was 11 m lower than it is today. During the maximum transgression, the relative sea level was about 0.75 m above the present level, and areas that are now land were covered by the sea. By using the Tudse Hage relative sea-level curve, combined with local morphological information (the seamless offshore/onshore morphological maps) the production of relevant paleogeographical maps reconstructing past shorelines is possible. These paleogeographical scenarios can digitally display any preferable time/depth to illustrate the possible paleogeography of a chosen archaeological setting. To show the strength of the paleogeographical maps, we have chosen the following scenarios: levels 8 m below present sea level (~8 cal. ka BP), 4 m below present sea level (~7.7 cal. ka BP), 2 m below present sea level (~7.4 cal. ka BP and possibly ~6.8 cal. ka BP), and 1 m above present sea level (~5.2 cal. ka BP). For each of these maps, terrestrial and archaeological finds relating to these periods were obtained from the Danish Heritage Agency's sites

and monuments record (http://www.kulturarv.dk/fundogfortidsminder/ accessed on 7 December 2021) and were overlain onto the maps.
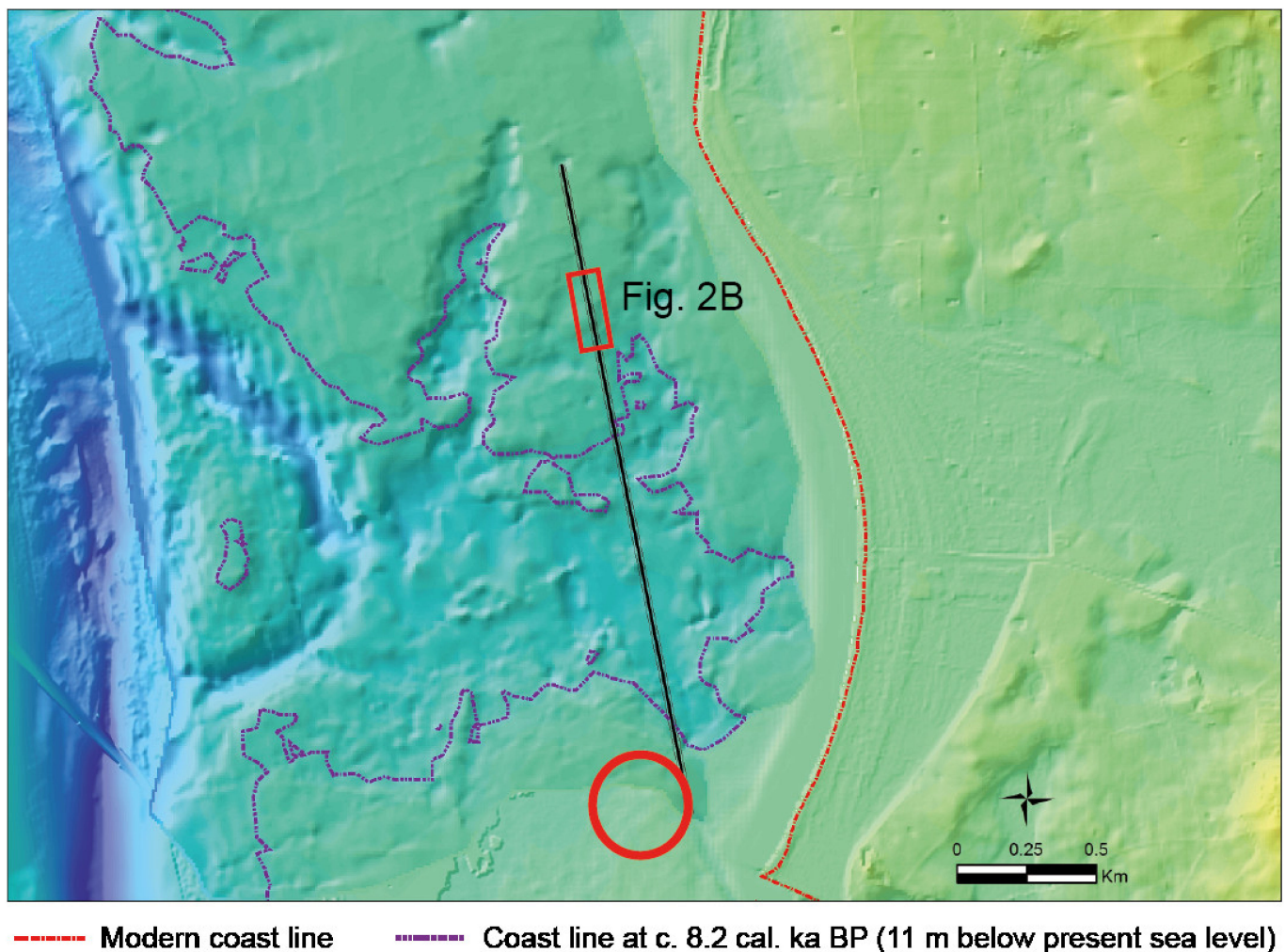

Figure 8. Paleogeographical map of the Tudse Hage area at a time when the relative sea level was 11 m lower than at present, corresponding to c. 8.2 cal. ka BP. The sediments that have accumulated after 8.2 ka have been "removed".

4.4. Geoarchaeological Paleogeographical Scenario 8 M below Present Sea Level (~8 Cal. Ka BP)

The "8 m below present sea level" scenario relates to the archaeological Kongemose culture, and the paleogeographical scenario (Figure 9A) shows that the sea level reached a transitional phase, from a previous channel phase to a transgression of the flat basin areas outside Tudse Hage. About 2 km northeast of Tudse Hage, an ellipse indicates the position of a small spit and a protected basin, a potential "hotspot area" for archaeological sites (Kongemose culture).

4.5. Geoarchaeological Paleogeographical Scenario 4 M below Present Sea Level (~7.7 Cal. Ka BP)

The "4 m below present sea level" scenario relates to the archaeological late Kongemose culture, and the paleogeographical scenario (Figure 9B) shows that the sea had transgressed most of the flat basin areas outside Tudse Hage. North of Tudse Hage, a till headland was exposed to erosion and the ellipse indicates the position of a possible hotspot area, with the formation of small spits and barriers, well-suited for settlement sites (late Kongemose culture).
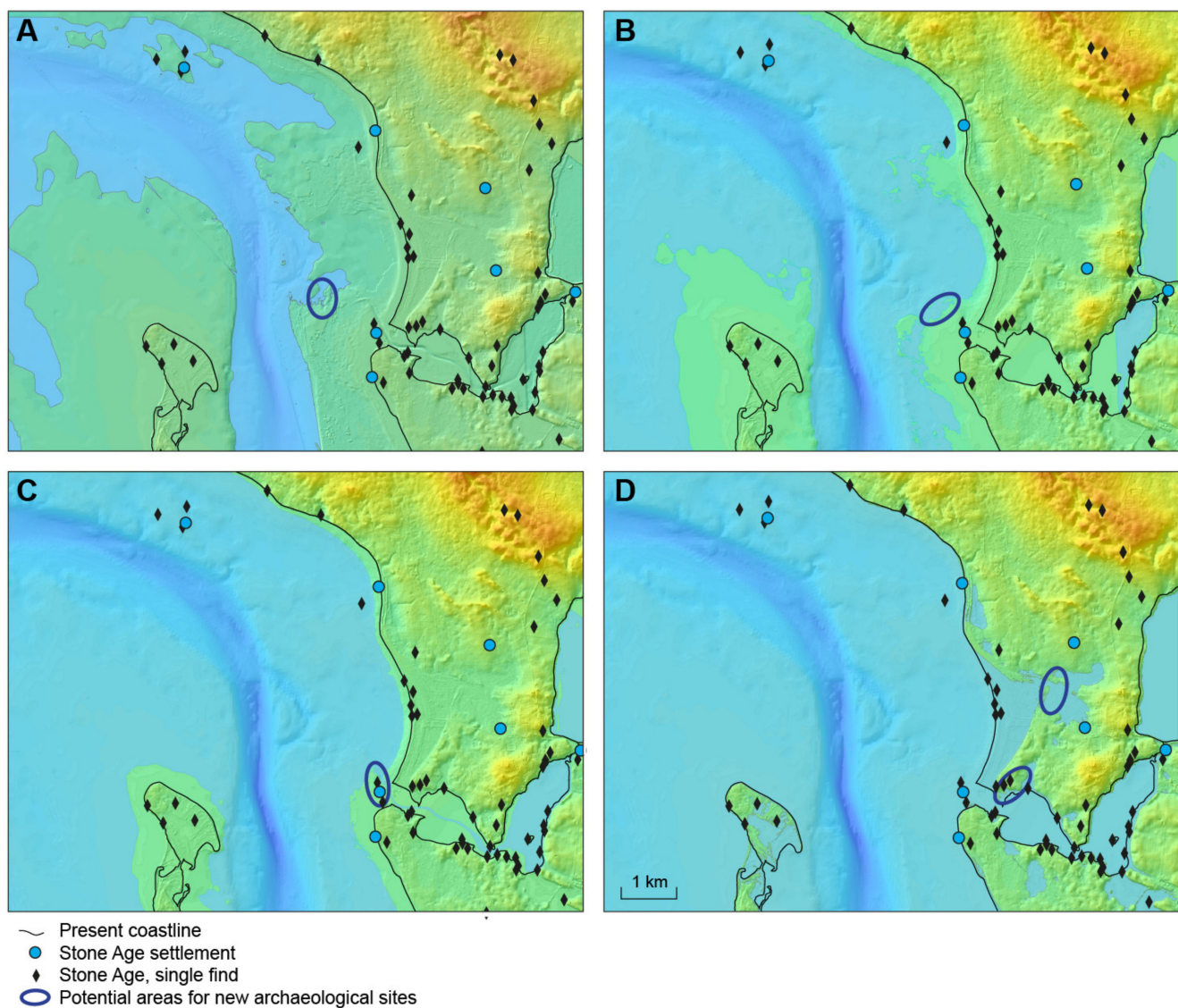
Figure 9. Geoarchaeological paleogeographical scenarios. (**A**) 8 m below present sea level (~8 cal. ka BP). (**B**) 4 m below present sea level (~7.7 cal ka BP). (**C**) 2 m below present sea level (~7.4 cal. ka BP and possibly ~6.8 cal. ka BP). (**D**) 1 m above present sea level (~5.2 cal. ka BP).

4.6. Geoarchaeological Paleogeographical Scenario 2 M below Present Sea Level (~7.4 Cal. Ka BP and Possibly ~6.8 Cal. Ka BP)

The "2 m below present sea level" scenario may be represented by two archaeological cultures because of a small regression shown on the sea-level curve (Figure 7). Finds from the archaeological Late Kongemose culture and the Ertebølle culture are both possible. The paleogeographical scenario (Figure 9C) shows that the Tudse Hage till headland was diminished. The ellipse indicates the position of a possible hotspot area, with the formation of a small spit; encouragingly, the main archaeological investigations ongoing at Tudse Hage fit with this hotspot.

4.7. Geoarchaeological Paleogeographical Scenario 1 M above Present Sea Level (~5.2 Cal. Ka BP)

The maximum transgression level of the Tudse Hage region is 0.75 m above the present sea level [17]. The detailed Danish onshore Digital Terrain Model reveals a system of spits and protected basins that was formed during the highest relative sea level, at about 5.5 cal ka BP in the Neolithic time period (Figure 9D). Two hotspot areas have been identified in relation to the spit formation and the sheltered basins.

4.8. Assessing the Preservation Potential of Sites

The established 2D time-series of the bottom current velocity and the current-generated bed shear-stress was gridded to a resolution of 50 m × 50 m and divided into two datasets, representing north- and south-going flow situations, and the temporal mean and maximum maps of each of the two flow situations were calculated. The annual maximum velocity maps of the north- and south-going current velocities are shown in Figure 10A,B, respectively. Knowing the current regimes and the seabed sediments, we can consider the ongoing sedimentary processes in the area. The Hjulström Diagram (Figure 11; [37]) shows the relationship between the sediment particle size and the velocity needed to erode, transport, or deposit sediments. The diagram shows the grain size on the horizontal axis, and the current velocity on the vertical axis, in a logarithmic scale. The two curves on the diagram represent the critical erosion velocity and the mean settling velocity. The critical erosion velocity curve shows the minimum velocity needed for the currents to erode (pick up) and transport materials of different sizes (as bedload or in suspension). Thus, a greater velocity is required to erode material compared to just transporting it. The mean settling velocity curve shows the velocities at which different-sized particles are deposited. Note that for coarser sediments (sand and gravel), it takes a slightly higher velocity to initially erode the particles than it takes to continue to transport them. For small particles (clay and silt), considerably higher velocities are required for erosion than for transportation, as these finer particles have cohesion resulting from electrostatic attractions. The diagram provides an approximation to the ongoing processes, but does not take into account the effects of rocks or boulders on the current flow, or biological growth, such as seagrass, which is known to stabilize and prevent seabed erosion [38]. The hydrodynamic model (Figure 10A,B) indicates that the annual north- and south-going bottom velocities reach 0.6–0.7 m/s and 0.8–0.9 m/s, respectively. The red box in Figure 11 shows the overall range in the Hjulström Diagram and indicates that the currents are sufficient to cause erosion and transport silt, sand, and some gravel. The strongest modelled currents, both north- and south-going, predominantly affect the southernmost part of the Tudse Hage area. A seabed sediment map for 2014 (http://www.geus.dk/UK/data-maps/jupiter/Pages/default.aspx accessed on 7 December 2021; Figure 10C) shows that the archaeological site currently lies in sand, which covers the culturally rich gyttja layers. The maximum modelled currents in the areas are in the order of 0.2–0.3 m/s and are thus capable of causing erosion and transport. Beyond this and going westwards, the seabed consists of glacial till, which is unlikely to be eroded. The observations taken when diving on the site reflect the modelled results. Cultural layers are capped with a fine layer of sand and gravel, which are mobile. In this area, the visibility was often poor because of the high turbidity caused by suspended particulate matter following strong winds. At the southwestern-most end of the site, very little gyttja survives, with the glacial till being directly covered by a layer of sand and fine gravel. As mentioned above, the modelling of the likely sediment transport is an approximation, as the Hjulström Diagram does not take into account the effects of seaweed/seagrass, which reduces erosion. Thankfully, there is a rich growth of seagrass over the archaeological area, which stabilizes the mobile sand and currently prevents the gyttja from being exposed and potentially eroded.
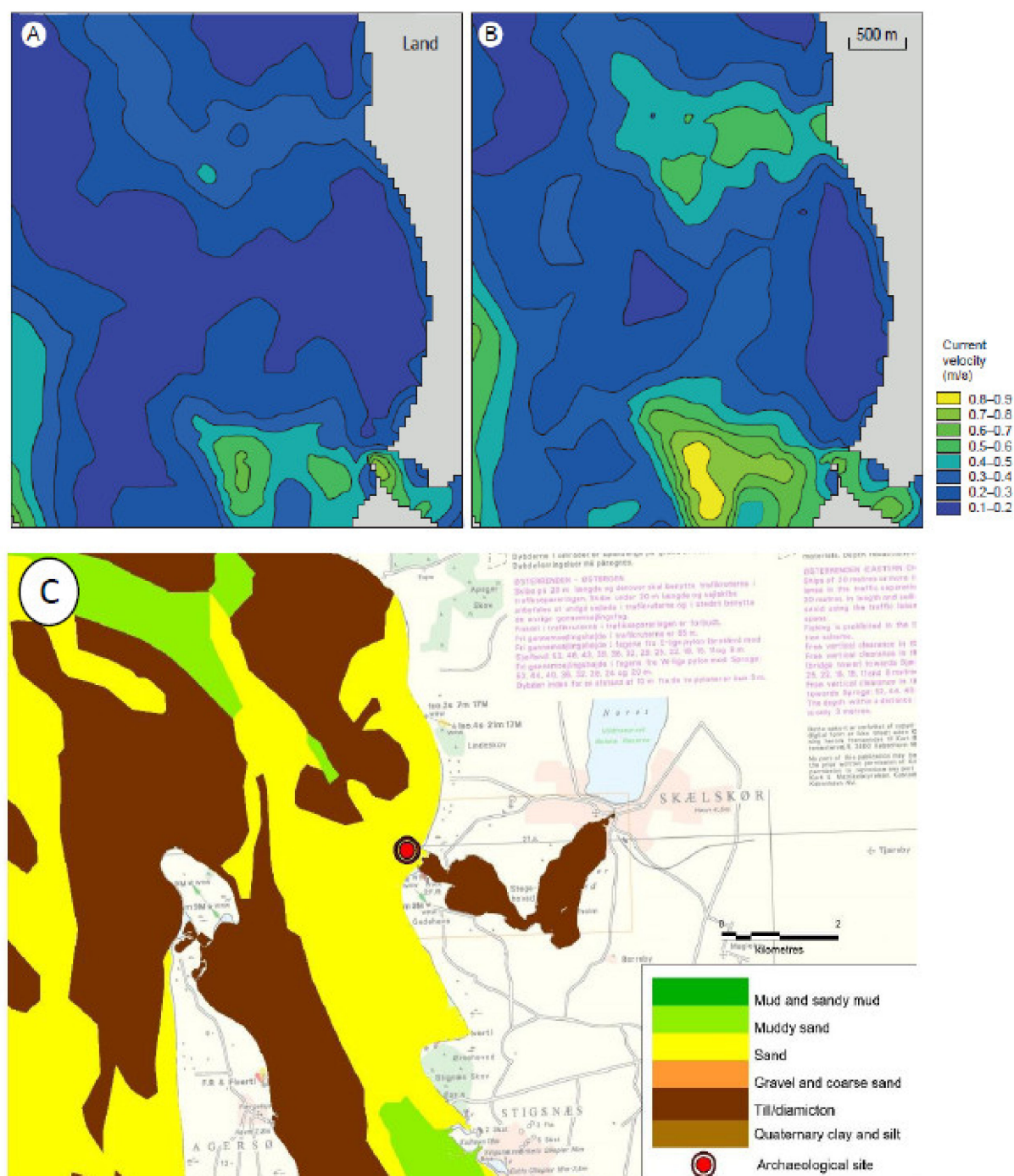
Figure 10. Annual maximum of modelled bottom current velocities (m/s). (**A**) north-going currents, (**B**) south-going currents, (**C**) seabed sediment map around Tudse Hage from 2014.
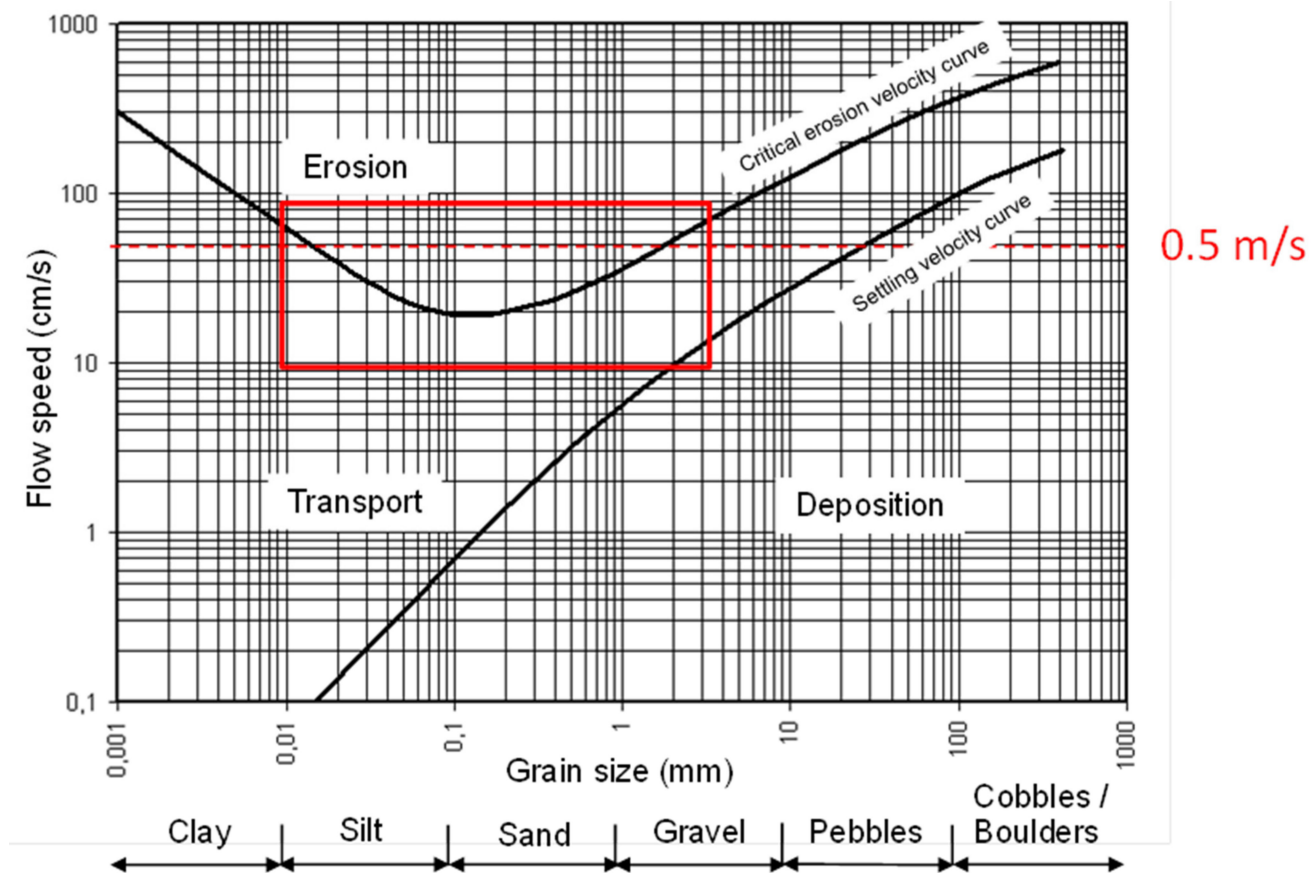
Figure 11. Hjulström Diagram. The red box indicates the range of modelled current velocities in the Tudse Hage area.

5. Conclusions

Locating the positions and extent of the submerged prehistoric sites and landscapes temporally and spatially is a key first step to answering archaeological research questions and managing this underwater cultural heritage. To address this, we have taken a downscaling and upscaling approach. Remotely gathered data from online databases and geophysical surveys, above and below the seabed, were collected and incorporated into a GIS to make seamless maps of the seabed and the sub-seabed surface morphology (downscaling). Key to the possibility of taking this approach is, in part: the online databases with marine/land data that are becoming increasingly available; the increased access to marine geophysics, or data that are collected as part of geotechnical surveys, in advance of subsea development; and, finally, the increased computing capacities and processing power of GIS software.

On the basis of these maps, sediment cores were taken from locations that would provide as wide a time span as possible for the evolution of the study area (upscaling). The sediments of the cores were described, macrofossils identified, and their ages determined by radiocarbon dating. In this manner, it was possible to model the relative sea-level change in the area and to assess which archaeological horizons are likely to have survived until today. For example, our results show that, in the Tudse Hage area, the lower and upper parts of the relative sea-level curve (Figure 7) are well-constrained from both terrestrial and marine ages, whereas the middle part is poorly constrained. We see evidence for an unconformity in the area, which could be due to a low stand, which may have occurred ~7.6 cal. ka BP. Furthermore, relative sea-level change can be extremely local—the curve developed here highlights how regional change has been in the past, and our results indicate that glacioisostatic rebound was more pronounced than in other nearby regions of Denmark. Thus, the down- and upscaling modelling approach taken here is extremely use-

ful for providing dateable evidence that can aid in the construction of the relative sea-level curves and the general evolution and survivability of the archaeological horizons/settings through the Holocene. On the basis of this, it was possible to use paleogeographical maps to reconstruct past shorelines. These paleogeographical scenarios can digitally display any preferable time/depth to illustrate the possible paleogeography of a chosen archaeological setting. The selection of hotspots, in our case, was based upon Fischer's original fishing-site-location model, which essentially takes into account the topography of the landscape and how this affects fishing. Critiques of this model express concern that it is based on assumptions about prehistoric resource-strategic behaviour that are oversimplistic and out-of-date in relation to the landscape ecology and the ethnographic and anthropological studies of current-day hunter-gatherer societies [6]. Nevertheless, we still maintain that it is of paramount importance to ascertain whether archaeological horizons still survive, on the basis of the geological evolution of an area. The model has currently only been validated to a limited extent. Diving in the areas represented in Figure 9A,B has yielded prehistoric finds from the Ertebølle period (The Viking Ship Museum, unpublished results, 2009/2011), and the area proposed in Figure 9C relates to the area where the known Tudse Hage site is found. However, further validation is required to discern if these are loose finds, settlement sites, or equally important, in this instance, evidence of paleocoastlines. A further element to the modelling work was to examine the effects of the environment on seabed erosion and the preservation of archaeological sites now, and in the future–current climate models predicate a global sea-level change of up to two metres by 2100, which will undoubtedly have an effect on seabed sedimentary processes. The seabed current/erosion model developed and the seabed map show that, in the majority of the Tudse Hage area, currents are not sufficient to significantly erode the present-day seabed. From the seabed map, it can also be seen that many areas are dominated by till deposits with a superficial covering of sand. Any deposits containing cultural material are unlikely to be preserved in these areas. Thankfully, the known site of Tudse Hage lies in an area where sand still caps the Holocene coastal deposits. This is reflected in what is seen on site, with the area where recent excavations were carried out still showing cultural deposits up to 70-cm thick. At the southernmost extent of the known site, Holocene coastal deposits have been eroded and glacial till dominates. This is exemplified by the remains of a fish trap that was being eroded from the seabed and that was stabilized in situ in the 1990s with sandbags, and that now sits on a small pedestal of gyttja, surrounded by a culturally sterile seabed.

References

1. Andersen, S.H. Shell middens ("Køkkenmøddinger") in Danish Prehistory as a reflection of the marine environment. In *Shell Middens in Atlantic Europe*; Milner, N., Craig, O.E., Bailey, G.N., Eds.; Oxbow Books: Barnsley, UK, 2007; pp. 31–45.
2. Benjamin, J. Submerged prehistoric landscapes and underwater site discovery: Reevaluating the 'Danish model' for international practice. *J. Isl. Coast. Archaeol.* **2010**, *5*, 253–270. [CrossRef]
3. Bennike, O.; Jensen, J.B. Postglacial relative shore level changes in Lillebælt, Denmark. *Geol. Surv. Den. Greenl. Bull.* **2011**, *23*, 37–40. [CrossRef]
4. Bennike, O.; Jensen, J.B.; Lemke, W.; Kuijpers, A.; Lomholt, S. Late and postglacial history of the Great Belt, Denmark. *Boreas* **2004**, *33*, 18–33. [CrossRef]
5. Bennike, O.; Nørgaard-Pedersen, N.; Jensen, J.B. The channels in Storebælt, Denmark: Implications of new radiocarbon ages. *Geol. Surv. Den. Greenl. Bull.* **2019**, *43*, e2019430106. [CrossRef]
6. Bierkens, P.M.F.; Finke, P.A.; Willigen, P.D. *Upscaling and Downscaling Methods for Environmental Research*; Kluwer Academic: Dordrecht, The Netherlands, 2000; pp. 354–355.
7. Christensen, C. Kystbesættelse og Havniveauændringer i Stenalderen. In *Danmarks Jægerstenalder–Status og Perspektiver*; Jensen, O.L., Sørensen, S.A., Hansen, K.M., Eds.; Hørsholm Egns Museum: Hørsholm, Denmark, 2001; pp. 183–193.
8. Christensen, C.; Fischer, A.; Mathiassen, D.R. Den Store havstigning i Storebælt. In *The Danish Storebælt Since the Ice Age-Man, Sea and Forest*; Pedersen, L., Fischer, A., Aaby, B., Eds.; A/S Storebæltsforbindelsen: Copenhagen, Denmark, 1997; pp. 45–54, 323–324.
9. Danish Hydraulic Institute (DHI). Effekt af næringssaltsreduktioner på miljøtilstanden i Karrebæk Fjord, Dybsø Fjord og Smålandsfarvandet, modelopsætning og scenarier. In *DHI Rapport for Landbrug og Fødevarer 05-2011*; Danish Hydraulic Institute (DHI): Hørsholm, Denmark, 2011.
10. Danish Hydraulic Institute (DHI). *MIKE 21 and MIKE 3 FLOW MODEL FM. Hydrodynamic and Transport. Module, Scientific Documentation*; Danish Hydraulic Institute (DHI): Hørsholm, Denmark, 2012.
11. Danish Museums Law. LBKnr 358 af 08.04.2014. The Danish Ministry of Culture, Copenhagen Denmark. 2014. Available online: https://www.retsinformation.dk/api/pdf/162504 (accessed on 7 December 2021).
12. FEHY. *Fehmarnbelt Fixed Link. Marine Water–Impact Assessment. Hydrography of the Fehmarnbelt Area*; DHI/IOW Consortium in association with LICengineering, Bolding and Burchard and Risø DTU. E1TR0058; Femern A/S: Copenhagen, Denmark, 2013; Volume II.
13. Fischer, A. *Stenalderbopladser På Bunden af Smålandsfarvandet. En Teori Afprøvet Ved Dykkerbesigtigelse [Stone Age settlements in the Småland Bight. A Theory Tested by Diving].*; Skov- og Naturstyrelsen: Hørsholm, Denmark, 1993.
14. Fischer, A. An entrance to the Mesolithic world below the ocean. Status of ten years'work on the Danish sea floor. In *Man and Sea in the Mesolithic*; Fischer, A., Ed.; Oxbow: Oxford, UK, 1995; pp. 371–384.
15. Fischer, A. People and the sea-settlement and fishing along the Mesolithic coasts. In *The Danish Storebælt Since the Ice Age-Man, Sea and Forest*; Pedersen, L., Fischer, A., Aaby, B., Eds.; Oxbow: Oxford, UK, 1997; pp. 63–77.
16. Fischer, A. Coastal fishing in Stone Age Denmark—Evidence from below and above the present sea-level and from the bones of human beings. In *Shell Middens and Coastal Resources along the Atlantic Facade, Held in York September 2005*; Milner, N., Craig, O.E., Bailey, G.N., Eds.; Oxbow: Oxford, UK, 2007; pp. 54–69.
17. Gregory, D. In situ preservation of marine archaeological sites: Out of sight but not out of mind. In *In Situ Conservation of Cultural Heritage: Public, Professionals and Preservation*; Richards, V., Mckinnon, J., Eds.; Flinders University: Adelaide, SA, Australia, 2019; pp. 1–16.
18. Gregory, D.; Manders, M. (Eds.) Best Practices for Locating, Surveying, Assessing, Monitoring and Preserving Underwater Archaeological Sites, SASMAP Guideline Manual 2. 2016. Available online: http://sasmap.eu/fileadmin/user_upload/temasites/sas_map/pdf/SASMAP_guideline_02_LR.pdf (accessed on 7 December 2021).
19. Grøn, O. Some problems with modelling the positions of prehistoric hunter-gatherer settlements on the basis of landscape topography. *J. Archaeol. Sci. Rep.* **2018**, *20*, 192–199. [CrossRef]
20. Heaton, J.T.; Köhler, P.; Butzin, M.; Bard, E.; Reimer, R.W.; Austin, W.E.N.; Ramsey, C.B.; Hughen, K.A.; Kromer, B.; Reimer, P.J.; et al. Marine20–the marine radiocarbon age calibration curve (0–55,000 cal BP). *Radiocarbon* **2020**, *62*, 779–820. [CrossRef]
21. Hjulström, F. Studies of the morphological activity of rivers as illustrated by the River Fyris. *Bull. Geol. Inst. Univ. Uppsalsa* **1935**, *25*, 221–527.
22. Houmark-Nielsen, M.; Linge, H.; Fabel, D.; Schnabel, C.; Xue, S.; Wilcken, K.M.; Binnie, S. Cosmogenic surface exposure dating the last deglaciation in Denmark: Discrepancies with independent age constraints suggest delayed periglacial landform stabilisation. *Quat. Geochronol.* **2012**, *13*, 1–17. [CrossRef]
23. ICOMOS. 1996. Available online: http://www.international.icomos.org/charters/underwater_e.pdf (accessed on 19 May 2021).
24. Jowsey, P.C. An improved peat sampler. *New Phytol.* **1996**, *65*, 245–248. [CrossRef]
25. Krause-Jensen, D.; Serrano, O.; Apostolaki, E.T.; Gregory, D.J.; Quesada, C.M.D. Seagrass sedimentary deposits as security vaults and time capsules of the human past. *Ambio* **2019**, *48*, 325–335. [CrossRef] [PubMed]
26. Kulturarvsstyrelsen. *Kulturarv en Værdifuld Ressource for Kommernes Udvikling*; Kulturarvsstyrelsen and Realdania: Copenhagen, Denmark, 2005.
27. Lotz, P. Tudse Hage—An underwater settlement on Sjælland. *Marit. Archaeol. Newsl. Rosk. Den.* **2000**, *14*, 8–13.

28. Lotz, P. Træ og træredskaber fra Tudse Hage. *Fund Fortid* **2011**, *3*, 4–8.
29. Lotz, P. Stenalderredskaber af træ fra Tudse Hage del 3. *Fund Fortid* **2012**, *1*, 8–11.
30. Lotz, P. *Tudse Hage–Bopladsen. Redskaber og Affald af Hjortetak, Knogle og Tand*, Unpublished report. 2016; p. 16.
31. Mertz, L. Oversigt over de sen- og postglaciale niveauforandringer i Danmark. *Dan. Geol. Undersøgelse II. Række* **2016**, *41*, 50. [CrossRef]
32. Missiaen, T.; Evangelinos, D.; Claerhout, C.; de Clercq, M.; Pieters, M.; Demerre, I. Archaeological prospection of the nearshore and intertidal area using ultra-high resolution marine acoustic techniques: Results from a test study on the Belgian coast at Ostend-Raversijde. *Geoarchaeology* **2018**, *33*, 386–400. [CrossRef]
33. Olsen, J.P.; Rasmussen, P.; Heinemeier, J. Holocene temporal and spatial variation in the radiocarbon reservoir age of three Danish fjords. *Boreas* **2009**, *38*, 458–470. [CrossRef]
34. Reimer, P.J.; Austin, W.E.; Bard, E.; Bayliss, A.; Blackwell, P.G.; Ramsey, C.B.; Butzin, M.; Cheng, H.; Edwards, R.L.; Friedrich, M.; et al. The IntCal20 Northern Hemisphere radiocarbon age calibration curve (0–55 cal kB). *Radiocarbon* **2020**, *62*, 725–757. [CrossRef]
35. Soulsby, R.L.; Clarke, S. Bed shear-stress under combined waves and currents on smooth and rough beds. In *Internal Report TR 137*; HR Wallingford: Manchester, UK, 2005; p. 52.
36. Stuiver, M.; Polach, H.A. Discussion of reporting ^{14}C data. *Radiocarbon* **1977**, *19*, 355–363. [CrossRef]
37. UNESCO Convention on the Protection of the Underwater Cultural Heritage. Available online: http://unesdoc.unesco.org/images/0012/001246/124687e.pdf#page=56 (accessed on 19 May 2021).
38. Valetta Treaty, Council of Europe. 1992. Available online: https://www.coe.int/en/web/conventions/full-list/-/conventions/treaty/143 (accessed on 19 May 2021).